



ORIGINAL ARTICLE

Experimental analysis of the structural behavior of different types of shear connectors in steel-concrete composite beams

Análise experimental do comportamento estrutural de diferentes tipos de conectores de cisalhamento em vigas mistas de aço-concreto

Juliano Geraldo Ribeiro Neto^a

Gregório Sandro Vieira^b

Rogers de Oliveira Zoccoli^c

^aRemy Consulting Engineers Toronto, Ontario, Canada

^bUniversidade Federal de Uberlândia – UFU, Faculdade de Engenharia Civil, Uberlândia, MG, Brasil

^cCentro Universitário Cathedral, Barra do Garças, MT, Brasil

Received 15 September 2019

Accepted 30 March 2020

Abstract: The present work aims to compare the structural behavior of steel-concrete composite-section beams for three types of shear connectors made of U hot rolled section and cold-formed sections of U and L. Experimental tests were performed with the three types of connectors associated with I section laminated steel beams and reinforced concrete slabs. For each type of connector, three push-out tests were performed, as well as six simple supported beam tests to evaluate the positive bending moment region. The results indicated that the direct shear behavior among the different types of connectors presents significant differences, however they do not significantly influence the average flexural strength of the composite beams. These, however, present considerable differences in deflections and deformations due to the stiffness differences of the connectors.

Keywords: push-out test, shear connectors, composite beams of steel and concrete.

Resumo: O presente trabalho tem como objetivo comparar o comportamento estrutural de vigas com seção mista de aço-concreto, para três tipos de conectores de cisalhamento, confeccionados em perfil laminado de seção U e em perfis metálicos formados a frio de seções U e L. Para tal, foram realizados ensaios experimentais com os três tipos de conectores associados a vigas metálicas em perfil laminado de seção I e lajes de concreto armado maciças. Para cada tipo de conector foram realizados três ensaios de cisalhamento direto, além de dois ensaios em vigas mistas simplesmente apoiadas para avaliação da região de flexão simples. Os resultados obtidos indicaram que o comportamento ao cisalhamento direto dos conectores apresenta diferenças expressivas a depender do modelo adotado, entretanto, não influenciam significativamente na capacidade resistente média à flexão das vigas mistas. Estas, contudo, apresentam diferenças consideráveis de deslocamento vertical e deformações em virtude das diferenças de rigidez dos conectores.

Palavras-chave: ensaio de cisalhamento, conectores de cisalhamento, vigas mistas aço-concreto.

How to cite: J. G. Ribeiro Neto, G. S. Vieira, and R. O. Zoccoli, “Experimental analysis of the structural behavior of different types of shear connectors in steel-concrete composite beams,” *Rev. IBRACON Estrut. Mater.*, vol. 13, no. 6, e13610, 2020, <https://doi.org/10.1590/S1983-41952020000600010>

1 INTRODUÇION

In several countries over the last few decades, steel-concrete composite structures have been increasingly used by engineering. In order to take advantage of the benefits of each material, both in structural and constructive terms, the composite steel-concrete elements are constituted by the combination of steel sections and concrete elements. The

Corresponding author: Juliano Geraldo Ribeiro Neto. E-mail: julianogeraldo.eng@gmail.br

Financial support: CNPq and Funape/UFU.

Conflict of interest: Nothing to declare.



This is an Open Access article distributed under the terms of the Creative Commons Attribution License, which permits unrestricted use, distribution, and reproduction in any medium, provided the original work is properly cited.

advantages of composite systems result from the fact that the steel and concrete elements can work subjected to tensile and compression efforts, respectively, a situation in which it is possible to explore the main mechanical properties of each material [1].

The search for more economical structural systems by reducing material consumption and the self-weight, without affecting their safety and durability, is one of the main objectives of structural engineering. The combination of steel and concrete in composite sections allows the complementation of the characteristics regarding both materials [2], which makes it possible to obtain elements of higher rigidity and smaller dimensions, providing a reduction in costs related to the foundation, resulting in performance and economy gains [3].

The interaction between the concrete elements and steel sections used in composite steel-concrete systems can be achieved by mechanical means (connectors, cavities, rebonds), by both friction and adhesion [4]. Although the natural adhesion between the two materials generates remarkably high friction forces, these are not usually considered when calculating the resistant capacity of some elements, such as composite beams [5].

The composite beams, in particular, are constituted by the association of a steel section located in a predominantly traction region with a concrete slab located in a prevalently compressed region. The mechanical connection among the materials is made by steel devices called shear connectors [4] whose main functions are: to allow the slab-beam elements to work together [3], to restrict longitudinal slipping and vertical displacement at the interface elements, in addition to absorbing shear forces [6].

The sizing of composite beams submitted to bending efforts depends on the characterization of the behavior at the level of the steel-concrete connection. Two situations are considered in this case: the complete and the partial interactions. When it comes to complete interaction, it is considered that there is a perfect connection between steel and concrete. In this case, there is no relative longitudinal slip between both elements. When slipping relative to the level of the steel-concrete connection occurs, there is a discontinuity regarding the deformation diagram characterizing the partial interaction [7].

The connection between steel and concrete is dimensioned according to the diagram of longitudinal shear forces per unit of length (q), known as longitudinal shear flow. In the case of complete interaction, the resultant of the longitudinal shear flow diagram (V_h) is given as a function of the maximum shear force that can be transferred through the connection, which is limited by the maximum tensile and compression resulting that may act on the steel beam and concrete slab, respectively. The number of connectors, when it comes to complete interaction, must then be determined to resist the resulting V_h [7].

When the resistant capacity of the connectors is higher or equal than the one of the components from the composite structure, (flow by tensile of the steel section or crushing by compression of the collaborative portion of the concrete slab), the degree of connection is total, in this case the connectors do not directly influence the flexural performance of the composite beam. If the resistance capacity of the connectors is less than the lowest resistance offered by either element, there is a partial connection, in which the connectors control the flexural strength of the composite beam [8].

In this context, it is known that the structural behavior of the connecting elements that acts on composite steel-concrete beams is a significantly important work, since their performance can directly compromise the safety and stability of the structures. The main idea of this article is to experimentally evaluate the efficiency of the connectors, checking the equivalence or the difference of the resistant capacity among the types of connectors analyzed.

By means of experimental tests, the work assessed the structural behavior of shear connectors made with three different steel sections associated with steel beams in laminated I section, connecting this to a reinforced concrete slab.

2 MATERIALS AND EXPERIMENTAL PROGRAM

The work consisted of analyzing the behavior of composite steel and concrete beams, double-based, subjected to forces applied at two points so that the central region was subjected to pure bending. All models with theoretical span equal to 2800 mm and two forces concentrated at a distance of 900 mm from each end, slab 800 mm wide and 100 mm thick (Figure 1).

Three different types of shear connectors were used, one in hot rolled U section and two in cold formed U and L sections, all welded to steel beams (Table 1).

For each type of shear connector, two identical parts were tested, differentiated by the nomenclatures "A", instrumented with electrical strain gauge, and "B", a reference piece.

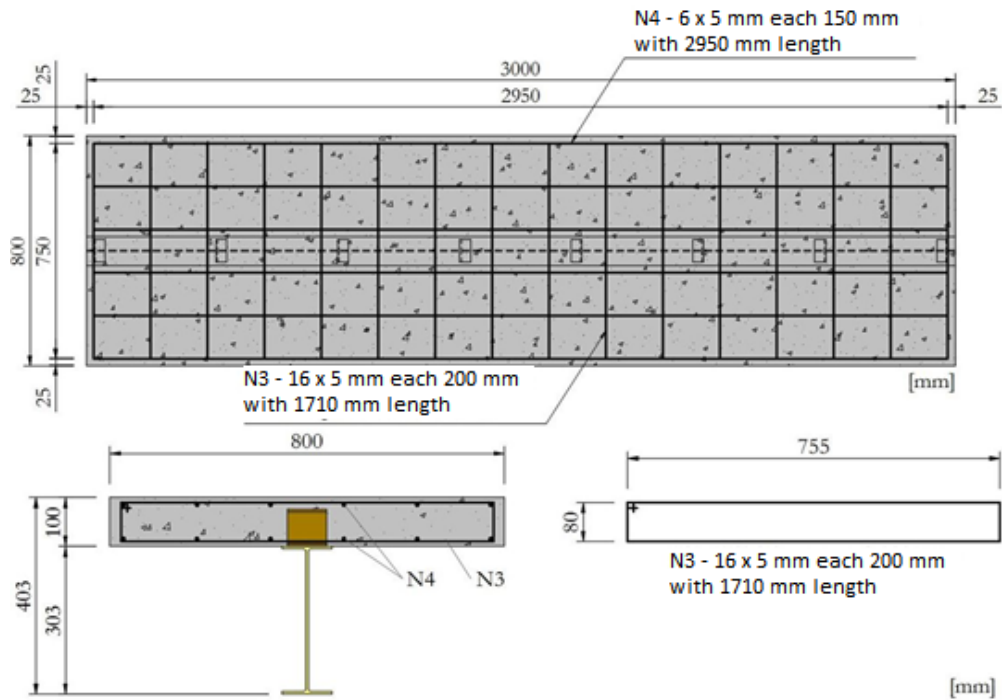


Figure 1. Beam dimensions and concrete slab reinforcement detail.

Table 1. Characterization of composite beam models

Beam	Steel beam section	Connector types	Connector
V1A*	W 310x21 (303x101x5.1x5.7)	U 3"x6.1	
V1B	W 310x21 (303x101x5.1x5.7)	U 3"x6.1	
V2A*	W 310x21 (303x101x5.1x5.7)	U 76x36x4.32	
V2B	W 310x21 (303x101x5.1x5.7)	U 76x36x4.32	
V3A*	W 310x21 (303x101x5.1x5.7)	L 76x36x4.32	
V3B	W 310x21 (303x101x5.1x5.7)	L 76x36x4.32	

* Beam and connectors instrumented with electrical strain gauges.

2.1 Materials Characterization

Two specimens were extracted from each type of section in order to obtain the mechanical properties of the steel from both the connectors and the beam. The ASTM A572-GR50, ASTM A36 and SAE 1020 steel specifications were used to make the beam, the hot rolled U section and for the cold formed U and L sections, respectively. The dimensions of the specimens met the minimum prescribed by the standard [9] (Figure 2). The elongation of the specimen was measured in accordance with the standard [10].

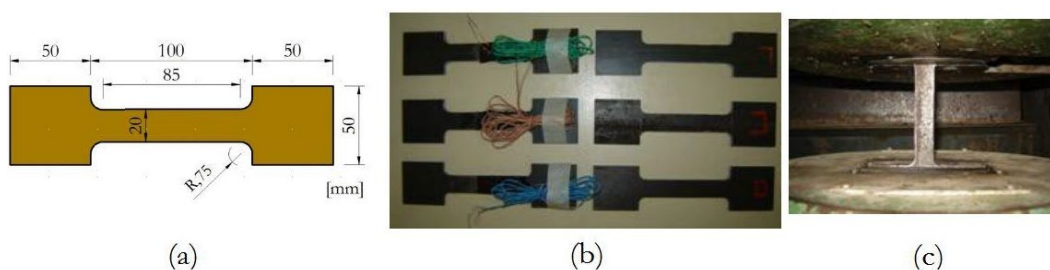


Figure 2. Steel specimen: (a) dimensions; (b) specimen; (c) on the testing machine.

The concrete used was machined and had a target value of 30 MPa with slump 12. All the slabs were concreted in a single step. After concreting, the strength gain of the concrete was monitored through tests to determine the compressive strength in twelve cylindrical specimens, measuring 10 x 20 cm (Figure 3), at 3, 7, 14 and 28 days. The modulus of elasticity and the tensile strength were also evaluated, all following the criteria of the respective standards [11]–[13].

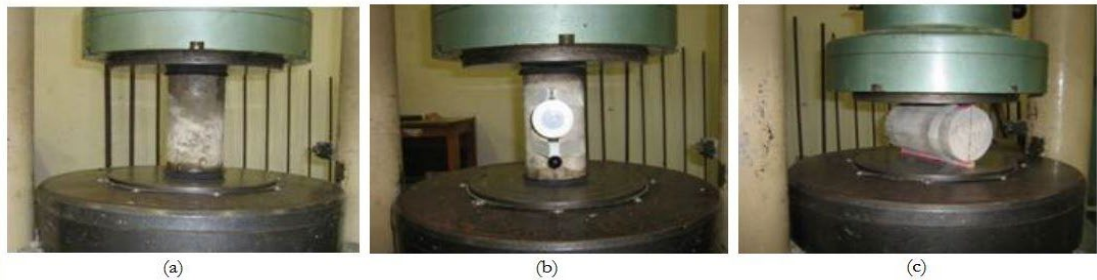


Figure 3. Concrete strength characterization test: (a) compression; (b) elastic modulus; (c) tension by diametral compression.

2.2 Connector testing (Push-out)

Three pieces were made for each type of shear connector, (Table 2), and only one of them was instrumented with electrical strain gauge. The dimensional characteristics and the arrangement of the reinforcements were in accordance with the criteria defined in the European standard [13] (Figures 4 and 5).

Table 2. Characterization of push-out test models

Model	Connector type	Length (mm)	Slab thickness ¹ (mm)	f_{c28,m^2} (MPa)
CD11	U 3"x6.1	80	100	30
CD12	U 3"x6.1	80	100	30
CD13*	U 3"x6.1	80	100	30
CD21	U 76x36x4.75	80	100	30
CD22	U 76x36x4.75	80	100	30
CD23*	U 76x36x4.75	80	100	30
CD31	L 76x36x4.75	80	100	30
CD32	L 76x36x4.75	80	100	30
CD33*	L 76x36x4.75	80	100	30

* Connectors instrumented with electrical strain gauges. ¹ Concrete slab. ² Target strength of concrete at 28 days

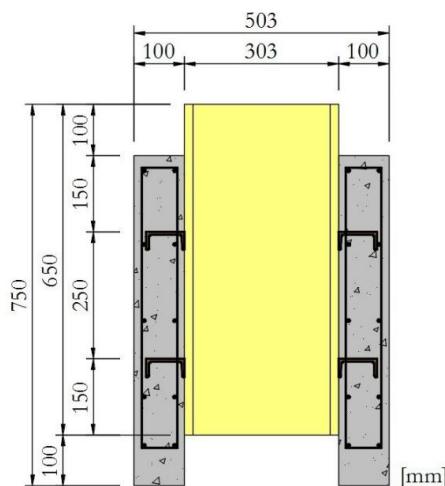


Figure 4. Push-out test models with shear connectors.

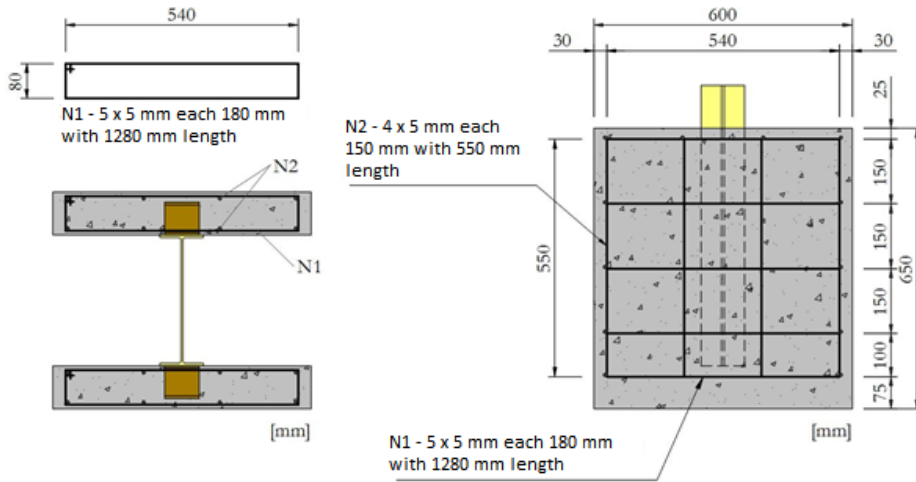


Figure 5. Concrete slab dimensions for push-out test models.

In order to measure the relative displacements between the beam and the slab, in addition to the distance between them, digital displacement meters were installed for this purpose (Figure 6). Steel uniaxial strain gauge was also installed in each connector (Figure 7), to measure the deformations and calculate the stresses.

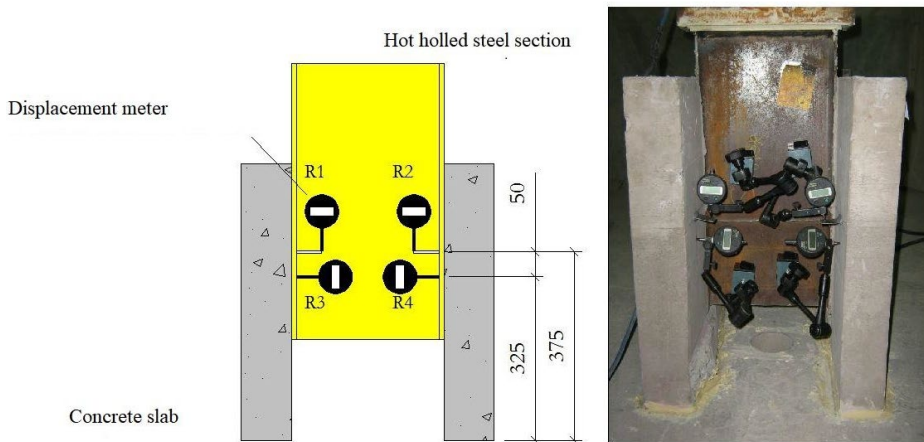


Figure 6. Positioning of displacement meters.

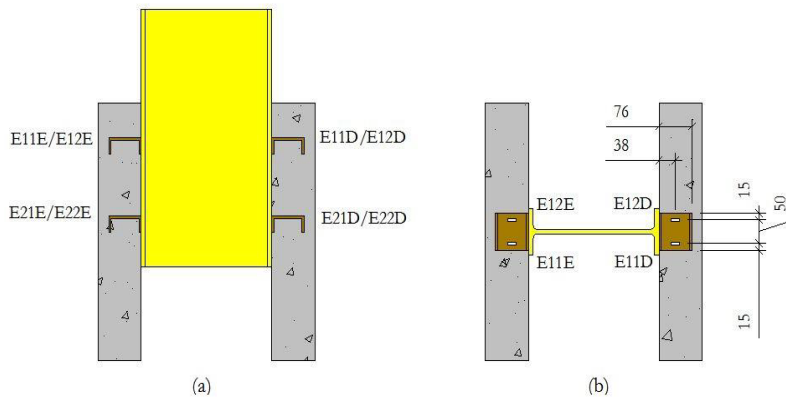


Figure 7. Positioning of shear connectors: (a) front view; (b) top view.

The force was applied directly to the steel section (Figure 8), with manual control of its application.



Figure 8. Test scheme for push-out.

2.3 Bending test on beams

Aiming to verify the structural behavior of the connectors acting directly at the interface of the steel beam with the concrete slab, two identical composite beams were made for each type of connector, where each pair differed from each other only by the presence of electrical strain gauge. The connectors were, except for those near the end of the beam, equally spaced respecting the maximum distance recommended by the standard [14] (Figure 9).

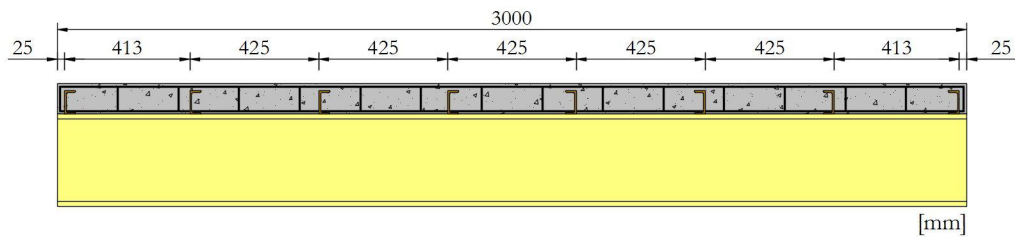


Figure 9. Positioning of shear connectors on the beam.

All beams tested for simple bending were instrumented by means of digital displacement meters, positioned in the middle and a quarter of the span (Figure 10). Such meters provided the information of relative horizontal displacement at the interface of the steel beam with the concrete slab, the same positioning points of the shear connectors (R1 to R4), and of the vertical displacement of the beam (R5 and R6).

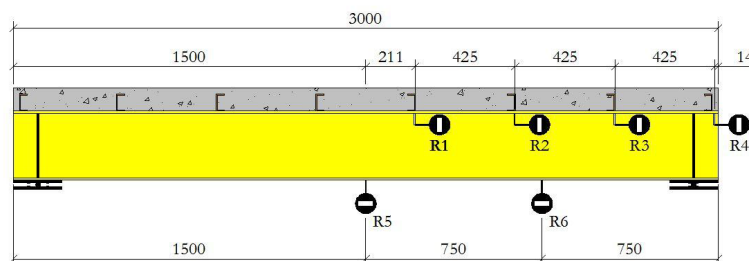


Figure 10. Positioning of the meter displacement.

The electrical strain gauge, uniaxial and rosettes, were positioned in order to obtain the deformations and to be able to calculate the stresses in both materials (Figures 11 and 12).

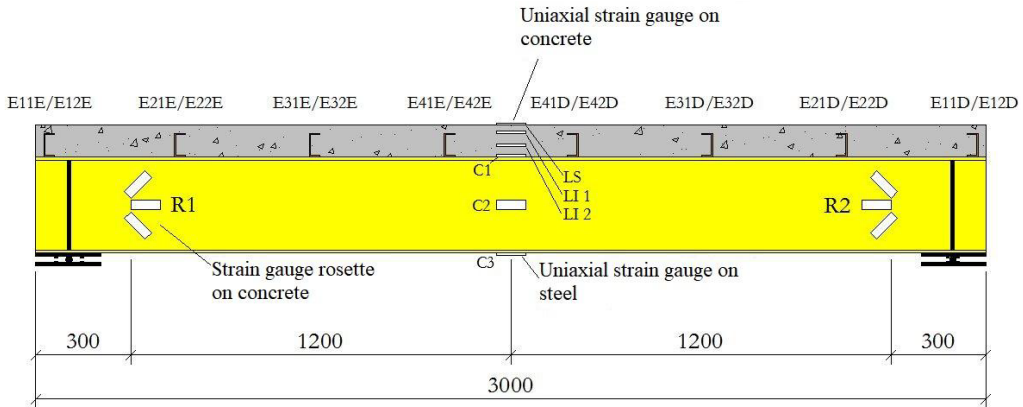


Figure 11. Side view of the positioning of the strain gauges on the beam.

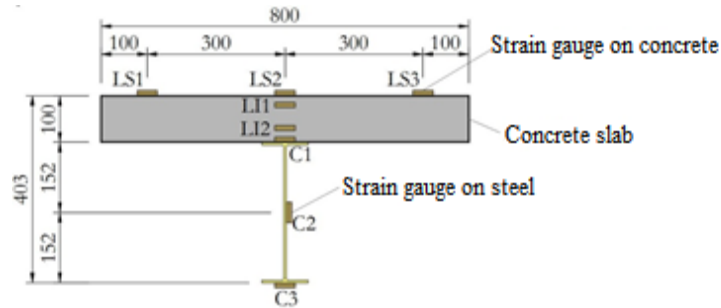


Figure 12. Cross section of the positioning of the strain gauges on the beam.

For flexural tests on composite beams, the same equipment used in the direct shear test was used (Figure 13).

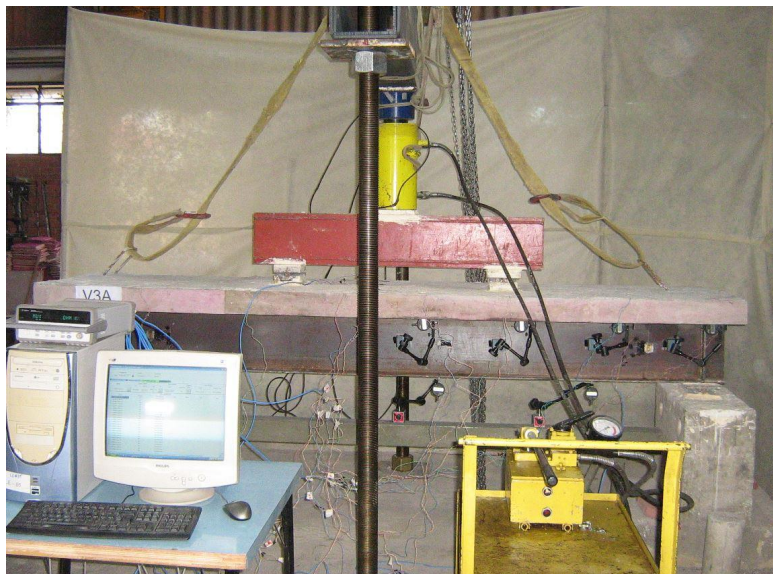


Figure 13. Test scheme for bending composite beam.

To guarantee the free displacement in the horizontal direction regarding the composite beam and the power transmission beam, by avoiding the appearance of efforts in this direction, steel plates and rollers were used (Figures 14 and 15).



Figure 14. Composite beam support.



Figure 15. Load transmission beam support.

3 RESULTS AND DISCUSSIONS

After testing the specimens, the values regarding the strength of the steel were used in the beams and connectors (Table 3).

Table 3. Steel Characterization

Specimen	Loads		Nominal (min.)		Experimental		A (%)	
	Yield (kN)	Ultimate (kN)	f_y (MPa)	f_u (MPa)	f_y (MPa)	f_u (MPa)		
U 3"x6.1 connector	CP1	37.4	58.3	250	400-550	306	478	26
	CP2	38.5	59.1			316	484	29
	Average	38.0	58.7			311	481	28
U 76x36x4.75 and L 76x36x4.75 connectors	CP3	22.0	40.1	210	380	231	422	28
	CP4	22.7	39.8			239	419	31
	Average	22.3	39.9			235	420	30
W310x21 steel beam	CP5	41.4	53.6	345	450	406	525	32
	CP6	42.4	54.2			416	531	28
	Average	42.0	53.9			411	528	30

The strength of the concrete over time until the day 28th after concreting as well as the values of resistance to compression, tensile and the modulus of elasticity of the concrete were obtained (Table 4). Apart from the compressive strength value, where the highest value was adopted, the tensile strength and the modulus of elasticity were obtained by averaging the results of three specimens.

Table 4. Concrete characterization

Compressive strength ABNT NBR-5739:2007 f_{cm} (MPa)				Tensile strength ABNT NBR-7222:1994 f_{ctm} (MPa)				Elastic modulus ABNT NBR-8522:2008 E_{cs} (GPa)			
Specimen		Higher		Specimen		Higher		Specimen		Higher	
CP1	CP2	CP3	Higher	CP1	CP2	CP3	Higher	CP1	CP2	CP3	Higher
32.7	33.9	35.0	35.0	3.2	3.2	3.1	3.2	33.1	34.5	32.6	33.4

3.1 Results of direct shear strength

In terms of the results about the push-out tests, the presented force refers to a connector.

Regarding the maximum resistant capacity per connector (Q_{max}) measurement, the lowest value obtained in the experiments was disregarded due to the significant variability that can occur among the values for the same type of connector. The average of the two highest experimental values has been adopted as a reference aiming to reduce the influence of possible spurious results in the analysis of the results, and the characteristic slip (δ_{uk}) was also evaluated. In order to measure the experiment, the results found were compared with the model proposed in the standard [15] for cold-formed and hot rolled U section, in addition to the model proposed by [16] for cold-formed U sections (Table 5).

From the results presented there is a significant variation in the resistant capacity among the different types of connectors. The laminated U sections connector presents a behavior similar to that already observed in other works [16]–[18]. The cold-formed U (CD2 series) and L (CD3 series) connectors have a lower resistant capacity when compared to the laminated U connector (CD1 series). This can also be observed by comparing the relative slip between the beam and the slab for each type of connector tested (Figure 16).

In almost all specimens it was observed that the cracks originated from the center of the slabs, propagating in two compression struts in relation to the largest dimension of the slab to the base (Figure 17).

3.2 Results of composite beams

Concerning the composite beams, the results are presented in graphs and tables, where the experimental values are compared with those analytically obtained. The mechanical properties considered for the analytical studies common to all beams are: concrete elastic modulus (E_c) equal to 33.4 GPa, characteristic concrete strength (f_c) equal to 35.01 Mpa, steel elastic modulus (E_a) equal to 200 GPa, steel yield stress (f_y) equal to 411 MPa and moment of inertia in relation to the beam flexion axis (I_a) equal to 3,776 cm⁴. Due to the variation of the connector type, the following parameters were obtained: beams V1A and V1B sum of resistance of the connectors ($\sum Q_n$) equal to 540 kN and degree of interaction (η) equal to 0.46, beams V2A and V2B summation resistance of connectors ($\sum Q_n$) equal to 360 kN and degree of interaction (η) equal to 0.32, beams V3A and V3B sum of resistance of connectors ($\sum Q_n$) equal to 290 kN and degree of interaction (η) equal to 0.26.

From the experimental values of the material properties, the elastic and plastic moments were calculated for comparison with the respective analytical values (Table 6). It is observed that, apart from beams with L section connectors, the others present an elastic experimental moment and coincide with the expected analytical values. Regarding plastic moment values, it is noted that the experimental values, although close, were lower than the analytical ones. However, this difference, below 5%, does not represent problems from the structural point of view, which is covered by the coefficients of safety indicated in the design standards.

In terms of maximum forces (Table 7), beams V1A and V1B, with connectors in laminated U-section and with an interaction degree equal to 0.46, cracked with 380 and 403 kN, respectively. The failure mode occurred due to concrete rupture in the region close to the point of the strength application, associated with the local buckling of the section (Figure 18). This is due to the increase in compression stresses in the upper region from the web section, after the loss of part regarding the contribution of slab in the resistant capacity of the component, because of its rupture.

Table 5. Maximum force and relative displacement for the different connectors

Connector	Model	Q _{máx.} (kN)	δ _{uk} (mm)	Q _{R,NBR} (kN)	Q _{R,DAVID} (kN)	$\frac{Q_{max}}{Q_{R,NBR}}$	$\frac{Q_{max}}{Q_{R,DAVID}}$	Rupture mode
U 3"x6,1	CD11	120.0	5.3	236	-	0.51	-	1
	CD12	135.0	2.7	236	-	0.57	-	1
	CD13	107.6	7.6	236	-	0.46	-	2
	Adopted	127.5	6.4	236	-	0.54	-	
U 76x36x4,75	CD21	87.6	4.1	184	166	0.47	0.53	1
	CD22	82.6	7.8	184	166	0.45	0.50	1
	CD23	92.5	8.8	184	166	0.50	0.56	3
	Adopted	90.1	8.3	184	166	0.49	0.54	
L 76x36x4,75	CD31	75.8	6.7	-	-	-	-	1
	CD32	69.3	2.0	-	-	-	-	1
	CD33	52.7	6.1	-	-	-	-	1
	Adopted	72.5	6.4	-	-	-	-	

-: not applicable
 1: excessive displacement
 2: weld failure
 3: weld failure near to shear connector area

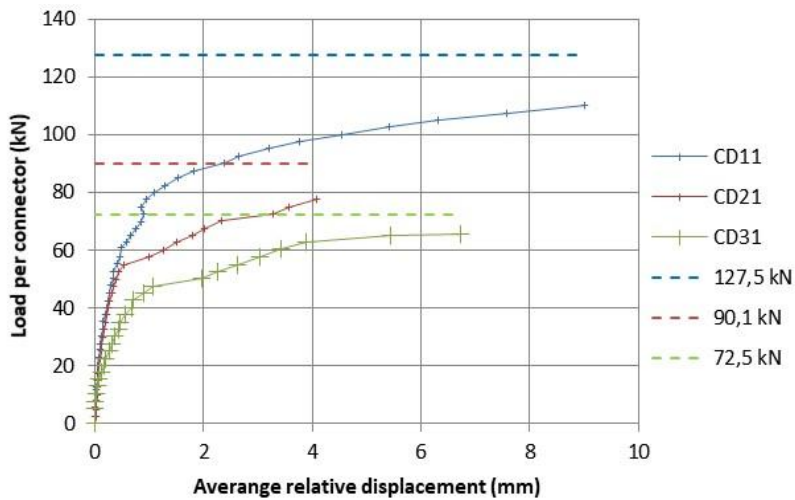


Figure 16. Curve load x average relative displacement per connector comparative between connectors.



Figure 17. Cracks on push-out models' slab.

Table 6. Resistant moments Experimental and analytical.

Beam	Experimental Elastic Moment (kN·cm) (1)	Experimental Plastic Moment (kN·cm) (2)	Analytical Elastic Moment (kN·cm) (3)	Analytical Plastic Moment (kN·cm) (4)	(1)/(3)	(2)/(4)	Rupture mode
V1A	15,607	17,407	15,568	18,232	1.00	0.95	1
V1B	15,697	18,442	15,568	18,232	1.01	1.01	1
V2A	14,707	17,407	14,718	17,717	1.00	0.98	2
V2B	14,797	17,182	14,718	17,717	1.01	0.97	2
V3A	12,142	14,437	14,259	16,816	0.85	0.86	3
V3B	13,357	15,652	14,259	16,816	0.94	0.93	3

Rupture mode:

1 – Concrete slab break with local web buckling
2 – Concrete slab break and steel beam yield
3 – Connector break and steel beam yield

Table 7. Experimental and analytical maximum load obtained for the beams.

Beams	Experimental maximum load (kN) - (1)	Analytical maximum load (kN) - (2)	$\frac{(1)}{(2)}$
V1A	380	405	0.94
V1B	403	405	1.00
V2A	380	394	0.96
V2B	375	394	0.95
V3A	314	374	0.84
V3B	341	374	0.91



Figure 18. Beam V1A rupture configuration.

For beams V2A and V2B, with U-shaped connectors formed by cold and the interaction degree of 0.32, rupture forces of 380 and 375 kN were obtained, respectively. The failure mode occurred due to the rupture of the concrete slab at the strength application point and the steel beam yield.

In the V3A and V3B beams, with cold-formed L- section connectors and 0.26 interaction degree, rupture forces of 314 and 340 kN were obtained (Figure 19). It was observed that the failure mode was characterized by the rupture of the connector, perceived during the test due to crackles heard inside the slab, followed by excessive vertical displacements due to the steel yield. Although a vertical separation between steel and concrete is not observed, this behavior suggests that the failure mode was characterized by the loss of the resistant capacity from the connectors, since the efforts are transferred to the steel beam and there is no collaboration of the concrete table.

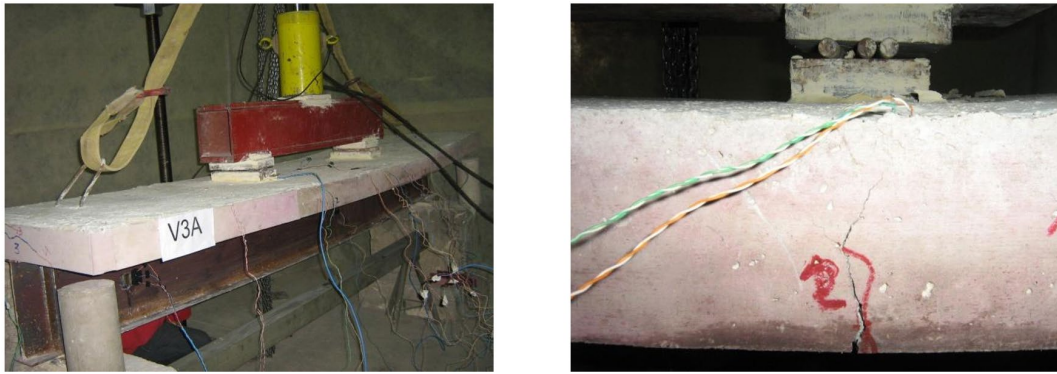


Figure 19. Beam V3A rupture configuration.

There was an attempt to analyze the relationship between the applied force and the deformation in the cross section in the middle of the span for four different loading values of 25, 50, 75 and 100% from the maximum force reached for the composite beams V1A to V3A (Figures 20 to 22).

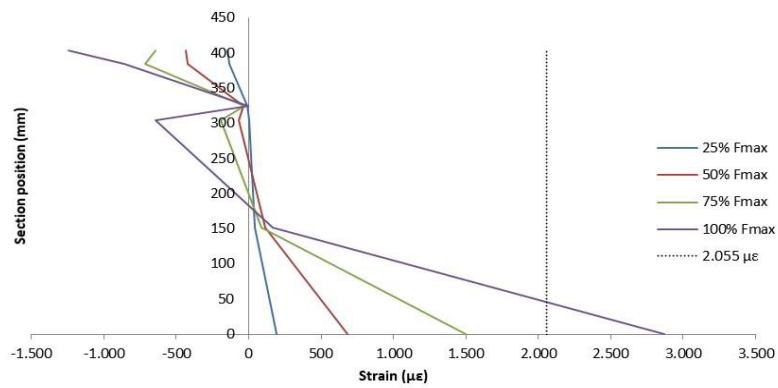


Figure 20. Strain distribution curve – V1A.

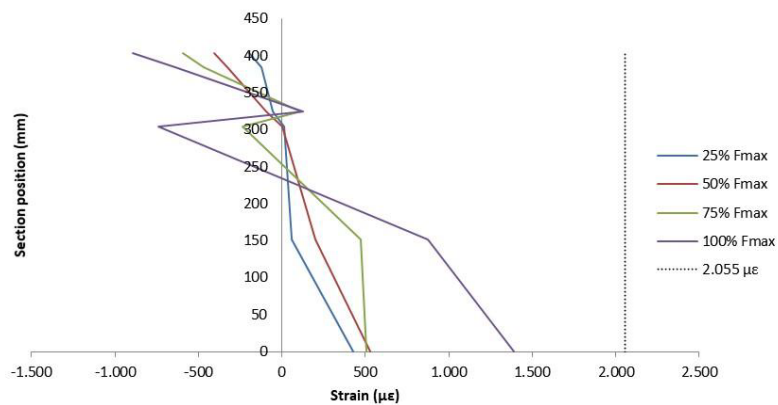


Figure 21. Strain distribution curve – V2A.

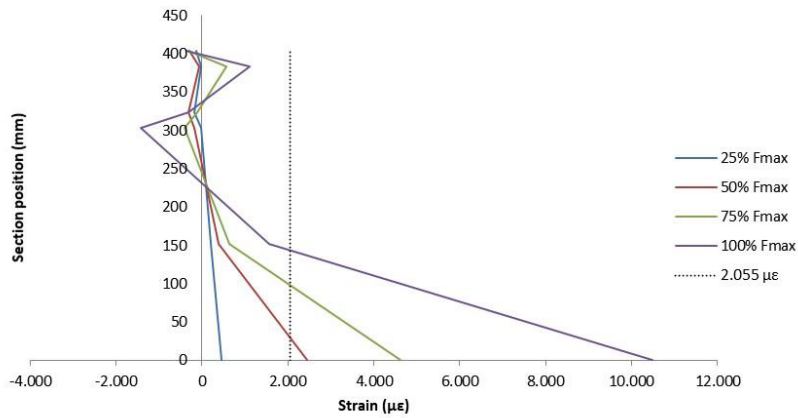


Figure 22. Strain distribution curve – V3A.

By analyzing the diagrams, the beam V1A (Figure 20) shows the existence of two neutral lines, one on the slab and one on the section, confirming the consideration of partial interaction. It is also verified that in the steel section the neutral line is in the web, confirming the theoretical analysis where the upper table of the section should be compressed.

The beam V2A (Figure 21) presents a behavior similar to the one of V1A, except for the fact that the most strained fiber of the steel section, represented by the point C3, does not reach the flow deformation. From the analysis of this beam, it is observed that after loading 180 kN, a stretch of decreasing deformations up to the force of 320 kN begins. It can be assumed that in this loading interval there was a loss of adhesion between the electrical strain gauge and the steel beam with later resumption of deformation growth. Thus, if we imagine that, contrary to what is shown by the measurements, in this stretch the deformations would continue to increase, it can be assumed that they would exceed the yield strength.

In beam V3A (Figure 22) it is observed that after 50% of the maximum load, a great loss of interaction occurs, which is possible to verify that the beam and the slab start to behave as if they were working in isolation. It is also observed that the deformations in the most stretched region of the steel section exceed considerably the yield deformation.

Another analyzed parameter was the relative displacement between the steel beam and the concrete slab, measured using digital displacement meters (Figure 10). These relative displacements were obtained by force readings at each 40 kN increment (Figures 23 to 25).

It was noted that the relative sliding between the slab and the section was practically null, while there was a bond between them. The force for which this bond was ruptured varied from beam to beam.

For beam V1A (Figure 23) the sliding measured by “R3” was higher than the sliding readings of other meters. This indicates a behavior of total interaction, considering that the interaction degree of this beam is 0.46, where the sliding in the region before the supports is much higher than the others.

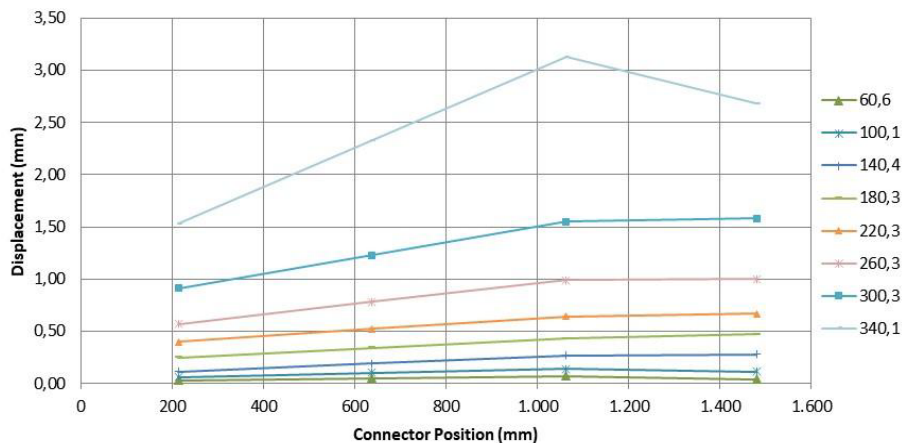


Figure 23. Relative displacement – V1A.

For the initial phase of the experiment, it is observed that the behavior of beams V2A (Figure 24) and V3A (Figure 25) is similar, with increasing displacements starting from the center towards the end, where the shear yield is higher. In the final phase of the experiment, close to the rupture, there is a change in the behavior of V3A, where it starts to present higher relative displacements in the center of the beam, a region where the shear yield is lower. Such behavior can be associated with the rupture of the connectors, generating a redistribution of efforts and a consequent increase in sliding.

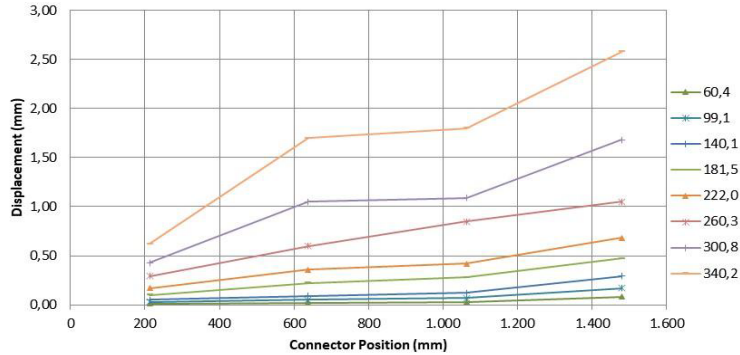


Figure 24. Relative displacement – V2A.

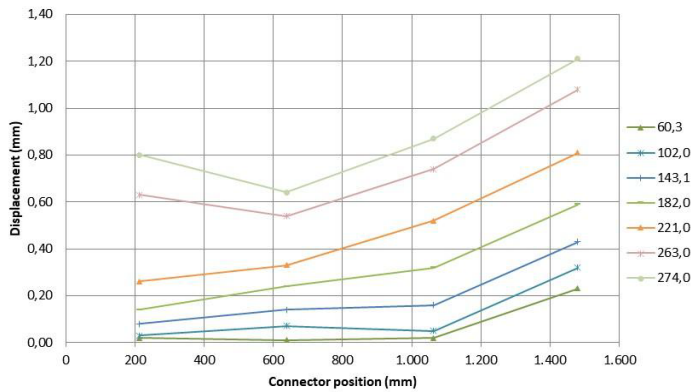


Figure 25. Relative displacement – V3A.

Comparing the relative sliding observed in the test of beams V1A, V2A and V3A (Figure 26), it is noted that the slides in the interface of the composite beams V2A and V3A present a similar behavior, although the beam V3A reached a lower force than V2A.

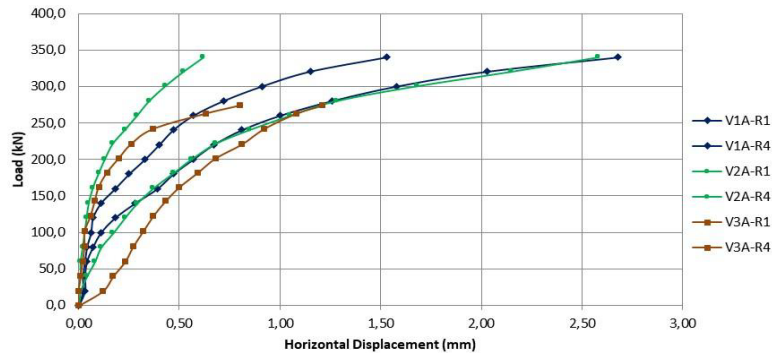


Figure 26. Comparative relative displacement curve – V1A, V2A e V3A.

Finally, the stress distribution in the connectors of the composite beams was analyzed (Figures 27 to 29). In general, the pairs of connectors positioned in symmetrical positions presented similar deformations.

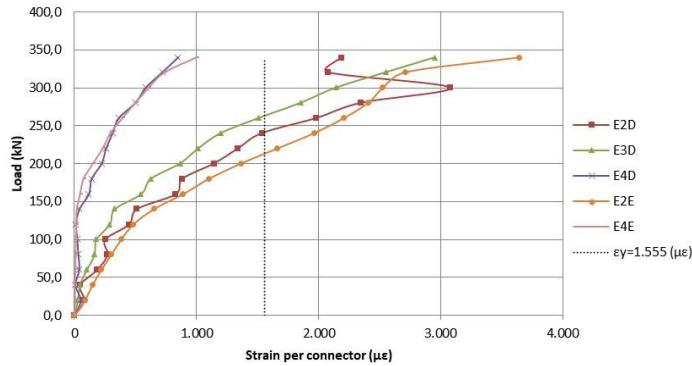


Figure 27. Load \times strain per connector curve – V1A.

For some connectors, at the place where the strain gauges were bonded, the deformations at the rupture moment of the beams were lower than the steel yield deformation (1555 $\mu\epsilon$ for cold rolled U connectors and 175 $\mu\epsilon$ for cold formed U and L). However, as noted by [16], the concentration of voltages in the connectors is higher at the base and it is approximately twice the voltage in the center of the connector. Thus, it can be concluded that even though the strain gauges bonded in the central region of some connectors have not registered deformations superior to the yield in the region with the highest concentration of stresses, along with the weld, probably there was the steel yield.

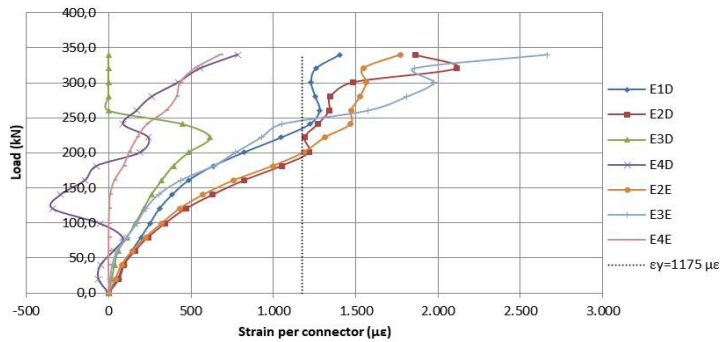


Figure 28. Load \times strain per connector curve – V2A.

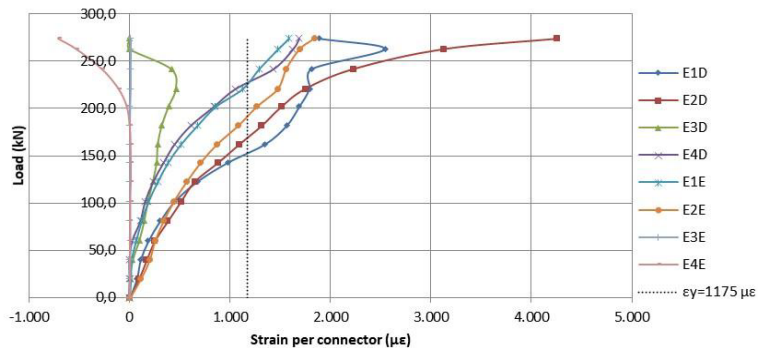


Figure 29. Load \times strain per connector curve – V3A.

It can also be seen that the highest deformations occurred in the connectors located in the symmetrical positions “2E” and “2D”, decreasing towards the central direction. Similarly, to the connectors of the push-out tests, those associated with the composite beams also showed deformations above the yield strength.

4 CONCLUSIONS

Motivated by the observation that in the execution of steel structures, the section replacement specified in the project with other equivalents is a common practice, as well as the fact that this replacement does not always meet a satisfactory equivalence of structural behavior, this research aimed to make a comparative study between the connectors in hot rolled U3”x6.1 and the cold formed U and L 76x36x4.75. For this purpose, push-out tests were performed to characterize the connectors, and also bending tests in composite beams to analyze the behavior of the connectors in a situation closer to the real one.

It was found that the U 3”x6.1 connector has a 46% higher resistant capacity than the U 76x36x4.75; and this in turn is 24% more resistant than the L 76x36x4.75. Comparing the hot rolled U and cold formed L sections, there is a 76% variation in the resistant capacity. The variation in stiffness between the sections proved to be directly associated with its resistant capacity, where the more resistant the section the more rigid it is, and smaller the relative sliding between the concrete slab and the steel section will be.

In almost all specimens, it was observed that the cracks originated in the center of the slabs, propagating in two compression struts compared with the largest dimension of the slab to the base. Some failure modes were not truly clear, suggesting that the concrete rupture may have occurred after excessive sliding of the connector.

It was also found that the resistant capacities obtained experimentally for hot rolled and cold formed U sections correspond to approximately half of the expected theoretical value. No justifications were found for this difference in resistant capacities, so these results are not conclusive about the application of such formulations since they have already been satisfactory in other studies [16], [18].

The relative sliding has a huge influence on the stiffness of the composite beams. For the beam with a higher degree of interaction, it was observed that the theoretical displacement was slightly higher than the experimental one. For beams with an interaction degree close to 0.3, the experimental displacements were, on average, close to the theoretical ones.

The relative sliding at the interface between the concrete slab and the steel section is null while there is a chemical bond between them and the force at which this bond is disrupted differs from beam to beam. It was also possible to verify that, despite the normative recommendation for uniform distribution of the shear connectors along the beam, the stress distribution is not constant and is concentrated at the ends.

Through the deformation diagram, the position of the neutral lines was obtained according to the loading steps, and it was possible to verify the influence of the interaction degree on the behavior of the composite beam and the plasticization of the cross section. For the L-type connector, it is noteworthy that, due to its higher flexibility and less resistance, there was less efficiency of the behavior as a composite beam with higher displacements and less resistance.

Regarding the composite beams, the relationship between the experimental resistant moment and the theoretical resistant moment ranged from 0.86 to 1.01, whose average was 0.95. This shows that the experimental outcomes of the beams presented results close to what was expected, suggesting that the experimental resistant capacities obtained for the connectors are corresponding to their behavior when associated with composite beams, although they are below the expected theoretical values.

Therefore, it is concluded that cold formed U and L sections can be used as shear connectors in composite beams, nonetheless their lower resistant capacities and stiffness, when compared to laminated U sections, must be taken into account in the project process. In situations of composite beams with high loading values or the need for high stiffness, as in structural systems subjected to dynamic actions, it is suggested that their use should be avoided. However, this study is not entirely conclusive, suggesting that more research needs to be carried out in order to better understand the behavior of the L section as shear connectors.

ACKNOWLEDGMENTS

The authors of this work would like to thank the CNPq funding agency, CAPES for the financial support. They also thank the extinct post-graduate program CMEC-UFG and UFG for laboratory support.

REFERENCES

- [1] G. S. Veríssimo, J. L. R. Paes, I. Valente, P. J. S. Cruz, and R. H. Fakury, "Design and experimental analysis of a new shear connector for steel and concrete composite structures," in *Proc. 3rd Int. Conf. Bridg. Maintenance, Saf. Manag. Bridg. Maintenance, Safety, Manag. Life-Cycle Perform. Cost*, 2006, p. 807–809.
- [2] M. D. A. Fabrizzi and R. M. Gonçalves, "Contribuição para o projeto e dimensionamento de edifícios de múltiplos andares com elementos estruturais mistos aço-concreto," M.S. thesis, Univ. São Paulo, São Carlos, 2008.
- [3] L. D. Kirchof, "Uma contribuição ao estudo de vigas mistas aço-concreto simplesmente apoiadas em temperatura ambiente e em situação de incêndio," M.S. thesis, Univ. São Paulo, São Carlos, 2004.
- [4] L. R. Marconcin, R. D. Machado, and M. A. Marino, "Modelagem numérica de vigas mistas aço-concreto," *Rev. IBRACON Estrut. Mater.*, vol. 3, no. 4, pp. 449–476, 2010, <http://dx.doi.org/10.1590/S1983-41952010000400006>.
- [5] J. G. R. Neto, "Análise teórico-experimental do uso de parafuso estrutural como conector de cisalhamento em pilar misto composto de perfil tubular preenchido com concreto," Ph.D. dissertation, Univ. Fed. Ouro Preto, Ouro Preto, 2016.
- [6] G. M. S. Alva and M. Malite, "Comportamento estrutural e dimensionamento de elementos mistos aço-concreto," *Cad. Eng. Estrut.*, vol. 7, pp. 51–84, 2005.
- [7] S.-H. Kim, S.-J. Park, W.-H. Heo, and C.-Y. Jung, "Shear resistance characteristic and ductility of Y-type perfobond rib shear connector," *Steel Compos. Struct.*, vol. 18, no. 2, pp. 497–517, 2015, <http://dx.doi.org/10.12989/scs.2015.18.2.497>.
- [8] D. J. Oehlers and M. A. Bradford, *Composite Steel and Concrete Structural Members – Fundamental Behaviour*, 1st ed. New York: Pergamon, 1995.
- [9] American Society for Testing and Materials, *Standard Test Methods and Definitions for Mechanical Testing of Steel Products*, A370, 1992.
- [10] Associação Brasileira de Normas Técnicas, *Materiais Metálicos – Ensaio de Tração à Temperatura Ambiente*, NBR ISO 6892, 2002, pp. 34.
- [11] Associação Brasileira de Normas Técnicas, *Concreto – Ensaio de Compressão de Corpos de Prova Cilíndricos*, NBR 5739, 2007, pp. 14.
- [12] Associação Brasileira de Normas Técnicas, *Concreto – Determinação dos Módulos Elásticos de Elasticidade e De Deformação à Compressão*, NBR 8522, 2008, pp. 16.
- [13] Associação Brasileira de Normas Técnicas, *Concreto e Argamassa – Determinação da Resistência à Tração por Compressão Diametral de Corpos de Prova Cilíndricos*, NBR 7222, 2011, pp. 8.
- [14] European Committee for Standardization, *Eurocode 4 – Design of Composite Steel and Concrete Structures – Part 1-1 – General Rules and Rules for Buildings*, 2004, pp. 118.
- [15] Associação Brasileira de Normas Técnicas, *Projeto de Estruturas de Aço e de Estruturas Mistas de Aço e Concreto de Edifícios*, NBR 8800, 2008, pp. 237.
- [16] D. L. David, "Análise teórica e experimental de conectores de cisalhamento e vigas mistas constituídas por perfis de aço formados a frio e laje de vigotas pré-moldadas," Ph.D. dissertation, Univ. São Paulo, São Carlos, 2007.
- [17] M. Malite, "Análise do comportamento estrutural de vigas mistas aço-concreto constituídas por perfis de chapa dobrada," Ph.D. dissertation, Univ. São Paulo, São Carlos, 1993.
- [18] I. A. Chaves, "Viga mista de aço e concreto constituída por perfil formado a frio preenchido," M.S. thesis, Univ. São Paulo, São Carlos, 2009.

Author contributions: JGRN: conceptualization, experimental study conduction, analysis and writing; GSV: experimental study conduction, analysis and writing; ROZ: analysis and writing.

Editors: Vladimir Guilherme Haach, José Luiz Antunes de Oliveira e Sousa, Guilherme Aris Parsekian.